Supplementary Information

for

Polymerizable Organo-gelator-stabilized Gel-emulsions Toward Preparation of Compressible Porous Polymeric Monoliths

Xuwei Fu, Pei Wang, Qing Miao, Kaiqiang Liu, Huijing Liu, Jianfei Liu and Yu Fang*

Key Laboratory of Applied Surface and Colloid Chemistry of Ministry of Education, School of Chemistry and Chemical Engineering, Shaanxi Normal University, Xi'an 710062, People's Republic of China

*E-mail: yfang@snnu.edu.cn; Tel: +86 29 81530786

Figure Captions and Table Legends:

Figure S1. ^{1}HNMR of CEA.

Figure S2. The HRMS of CEA.

Figure S3. ^{1}HNMR of D-PDMS.

Scheme S1. The structure of the fluorescence probe employed.

Table S1. Appearances, T_{gel} values (°C) and CGCs (%; in parentheses) of CEA (2.5%, *w/v*) in different solvents

Figure S4. Images of gel-emulsions with six gelled solvents (60 μL) in the oil phase: (a) *n*-pentane, (b) *n*-hexane, (c) *n*-heptane, (d) *n*-octane, (e) *n*-nonane, (f) cyclohexane (the basic composition of the system: 2% CEA in the organic phase, toluene: 40 μL, and water: 0.9 mL.

Figure S5. Microstructure of gel-emulsions with different volume ratios of *n*-heptane to toluene: (a) gel, (b) 10:0, (c) 9:1, (d) 8:2, (e) 7:3, (f) 6:4, (j) 5:5 (CEA concentration in the organic phase 2 *wt*%, water content 90%).

Figure S6. Evolution of *G'* as a function of the applied shear stress at different ratios of *n*-heptane to toluene in the continuous phase. The fundamental composition of the gel-emulsions is: CEA (3%, *w/v*, volume of the continuous phase), volume ratio of the continuous phase to that of the dispersed phase is 1:9.

Figure S7. Images of the monoliths prepared from gel-emulsions with different contents of CEA: (a) 2% CEA (*w/v*), (b) 2.5% CEA, (c) 3% CEA, (d) 3% CEA, 1 mg hydrophobic SiO_2 (the basic composition of the system: D-PDMS: 0.075 g, AIBN: 2 mg, toluene:40 μL, *n*-heptane: 60 μL, and water: 900 μL).

Figure S8. FTIR spectra of the monoliths, where (a, b) are the images of monolith c and d (c.f. Figure S7) respectively.

Figure S9. TGA curves for monolith d (c.f. Figure S7).

Figure S10. SEM micrographs of the monoliths prepared by the polymerization of corresponding gel-emulsions of the volume ratio of *n*-heptane to toluene (*v:v):* (a) 10:0; (b) 9:1; (c) 8:2; (d) 7:3; (b) 6:4; (f) 5:5; (the basic composition of the system: CEA: 3% of the organic phase (*v/v*), D-PDMS: 0.075 g, AIBN: 2 mg, 1 mg hydrophobic SiO_2 and water: 0.9 mL).

Figure S11.Pore diameter distribution of dried samples of the monolith d (c.f. Figure S7d).

Figure S12. The real traces of the time-dependent adsorptions of the as prepared porous monolith (FigureS7d) and the commercially obtained ACs to (a) toluene and (b) formaldehyde.

Figure S13. Variation of Wt/W_e versus time for toluene (a) and formaldehyde adsorption on monolith **d** (c.f. figure S7)

Figure S14. Images of contact angles of two porous materials with water, where (a, b) are the images of monoliths **c** and **d** (c.f. Figure S7), respectively.

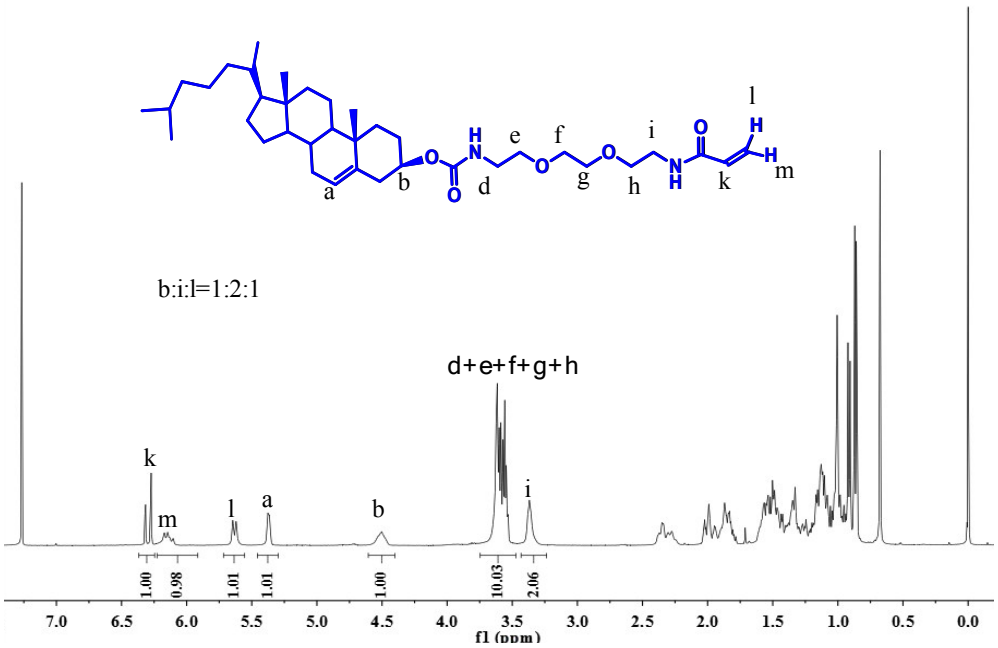

Figure S1. [1]HNMR of CEA .

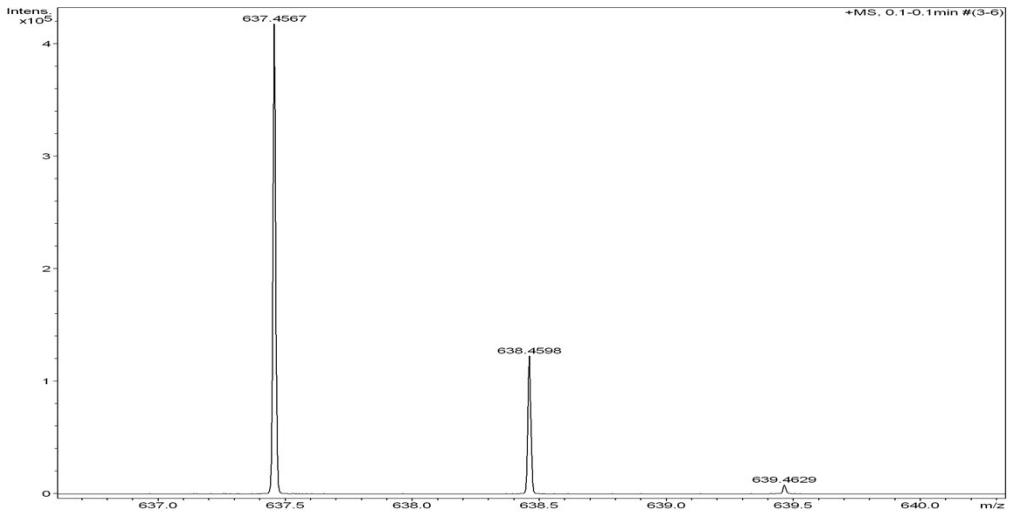

Figure S2. The HRMS of CEA.

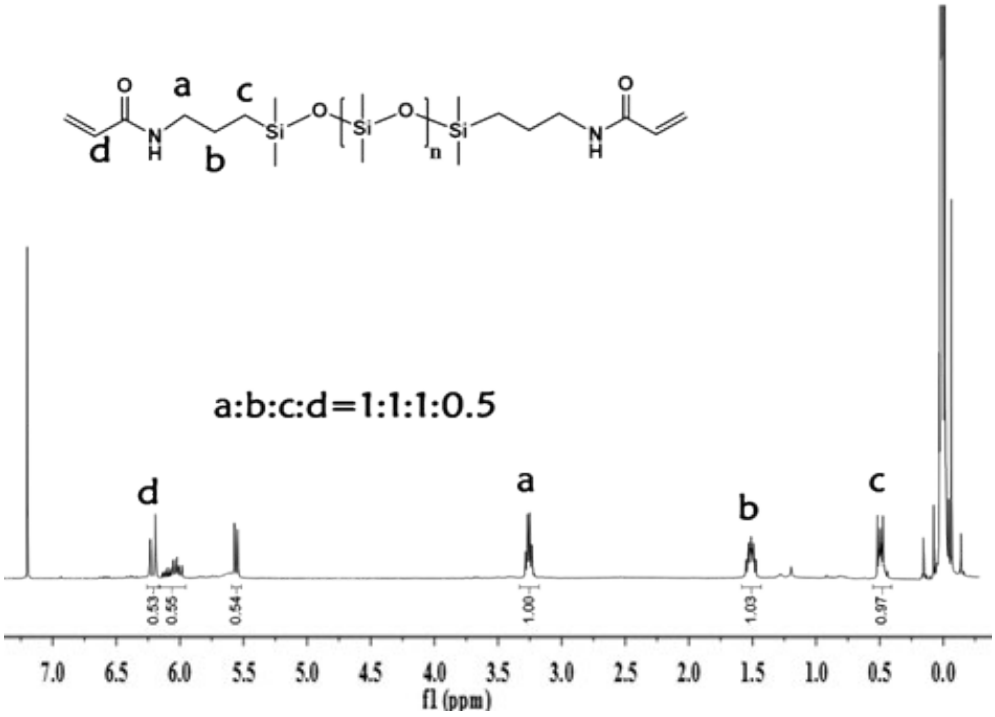

Figure S3. [1]HNMR of D-PDMS

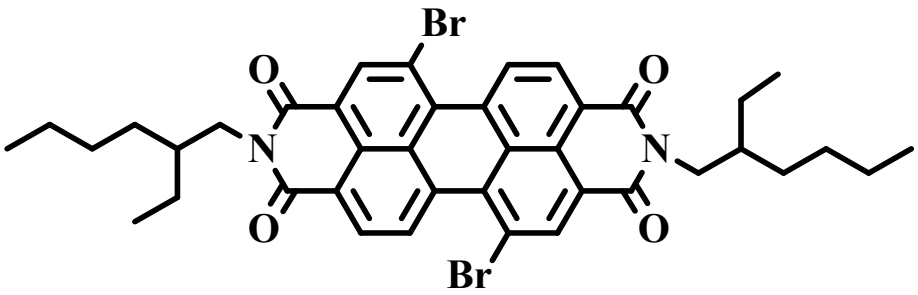

Scheme S1. The structure of the fluorescence probe employed.

Table S1. Appearances, T_{gel} values (°C) and CGCs (%; in parentheses) of CEA (2.5%, *w/v*) in different solvents

Solvent	CEA	Solvent	CEA	Solvent	CEA	
methanol	S	$CHCl_3$	S	*n*-hexane	G, ~42 (2) [a]	
ethanol	S	ethyl ether	P	*n*-heptane	G, ~76 (1)	
n-propanol	S	petroleum ether	I	*n*-octane	G, ~74 (0.5)	
n-butanol	S	benzene	S	*n*-nonane	G, ~68 (0.1)	
n-pentanol	S	toluene	S	*n*-decane	G, ~80 (0.05)	
n-hexanol	S	acetic acid	S	cyclohexane	PG	
n-heptanol	S	acetonitrile	P	THF	S	
cyclohexanol	S	TEA	P	acetone	S	
CCl_4	S	DMSO	S	ethyl acetate	P	
H_2O	I	DMF	S	pyridine	S	
methyl acrylate	S	methyl methacrylate	S	*n*-buty acrylate	S	
vinyl cyanide	S	styrene	S	*t*-butyl methacrylate	P	

S = Solution; P = Precipitation; I = Insoluble; G = Gel; PG = partial gel.

[a] 42 (2) means that the T_{gel} (transition temperatures of gel-sol phase) of the gel system is 42°C and the CGC (critical gelation concentration) is 2% (*w/v*).

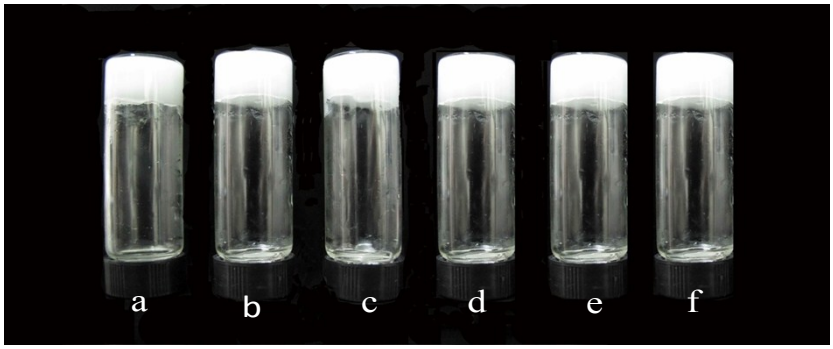

Figure S4. Images of gel-emulsions with six gelled solvents (60 μL) in the oil phase: (a) *n*-pentane, (b) *n*-hexane, (c) *n*-heptane, (d) *n*-octane, (e) *n*-nonane, (f) cyclohexane (the basic composition of the system: 2% CEA in the organic phase, toluene: 40 μL, and water: 0.9 mL.

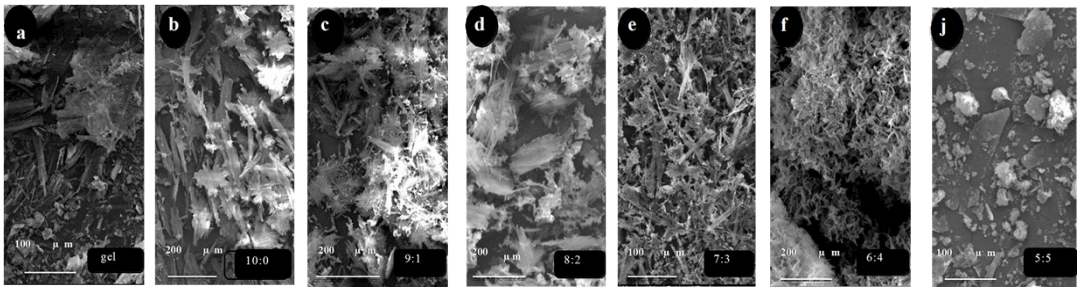

Figure S5. Microstructure of gel-emulsions with different volume ratios of *n*-heptane to toluene: (a) gel, (b) 10:0, (c) 9:1, (d) 8:2, (e) 7:3, (f) 6:4, (j) 5:5 (CEA concentration in the organic phase 2 *wt*%, water content 90%).

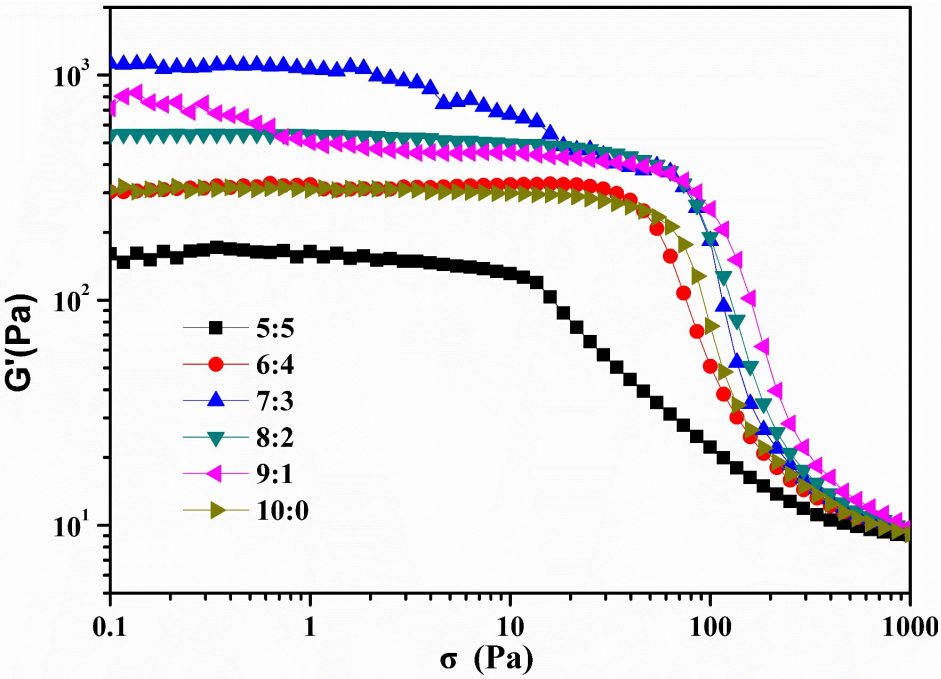

Figure S6. Evolution of *G'* as a function of the applied shear stress at different ratios of *n*-heptane to toluene in the continuous phase. The fundamental composition of the gel-emulsions is: CEA (3%, *w/v*, volume of the continuous phase), volume ratio of the continuous phase to that of the dispersed phase is 1:9.

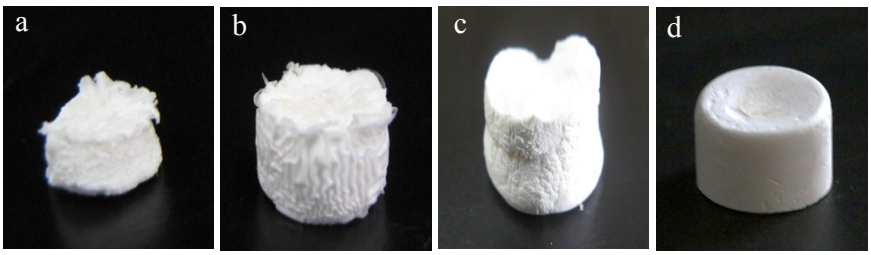

Figure S7. Images of the monoliths prepared from gel-emulsions with different contents of CEA: (a) 2% CEA (*w/v*), (b) 2.5% CEA, (c) 3% CEA, (d) 3% CEA, 1 mg hydrophobic SiO_2 (the basic composition of the system: D-PDMS: 0.075 g, AIBN: 2 mg, toluene:40 μL, *n*-heptane: 60 μL, and water: 900 μL).

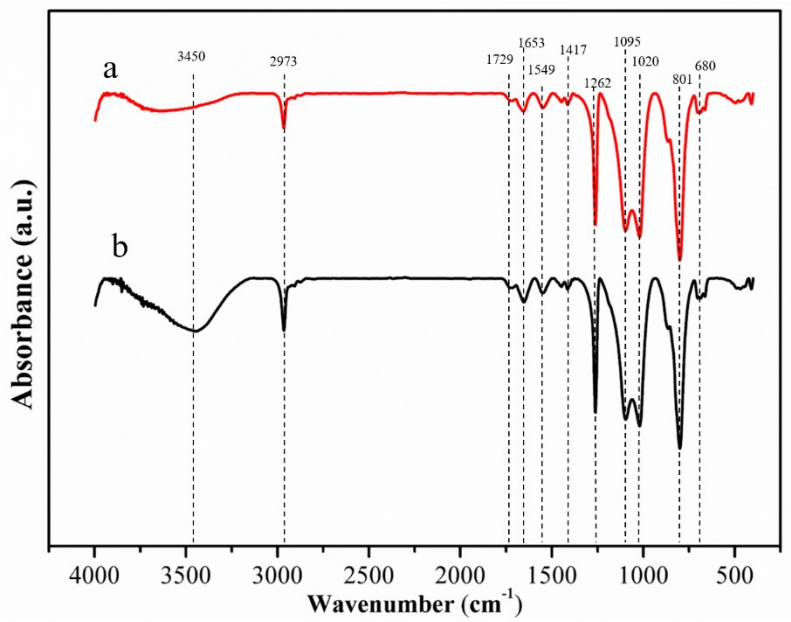

Figure S8. FTIR spectra of the monoliths, where (a, b) are the images of monolith c and d (c.f. Figure S7) respectively.

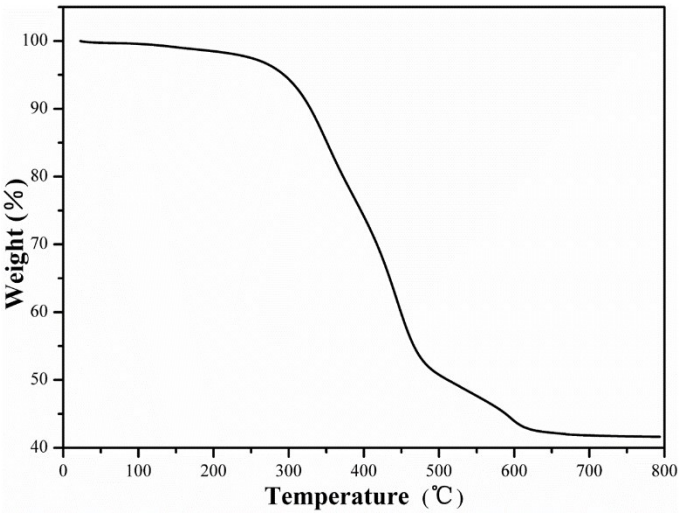

Figure S9. TGA curves for monolith **d** (c.f. Figure S7)

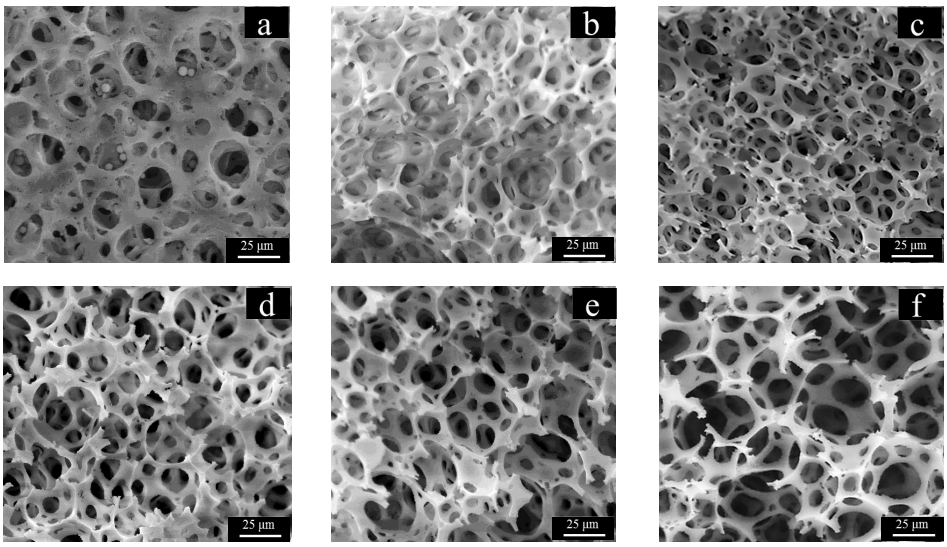

Figure S10. SEM micrographs of the monoliths prepared by the polymerization of corresponding gel-emulsions of the volume ratio of *n*-heptane to toluene (*v:v):* (a) 10:0; (b) 9:1; (c) 8:2; (d) 7:3;(b) 6:4; (f) 5:5; (the basic composition of the system: CEA: 3% of the organic phase (*v/v*), D-PDMS: 0.075 g, AIBN: 2 mg, 1 mg hydrophobic SiO_2, organic phase: 0.1 mL, and water: 0.9 mL).

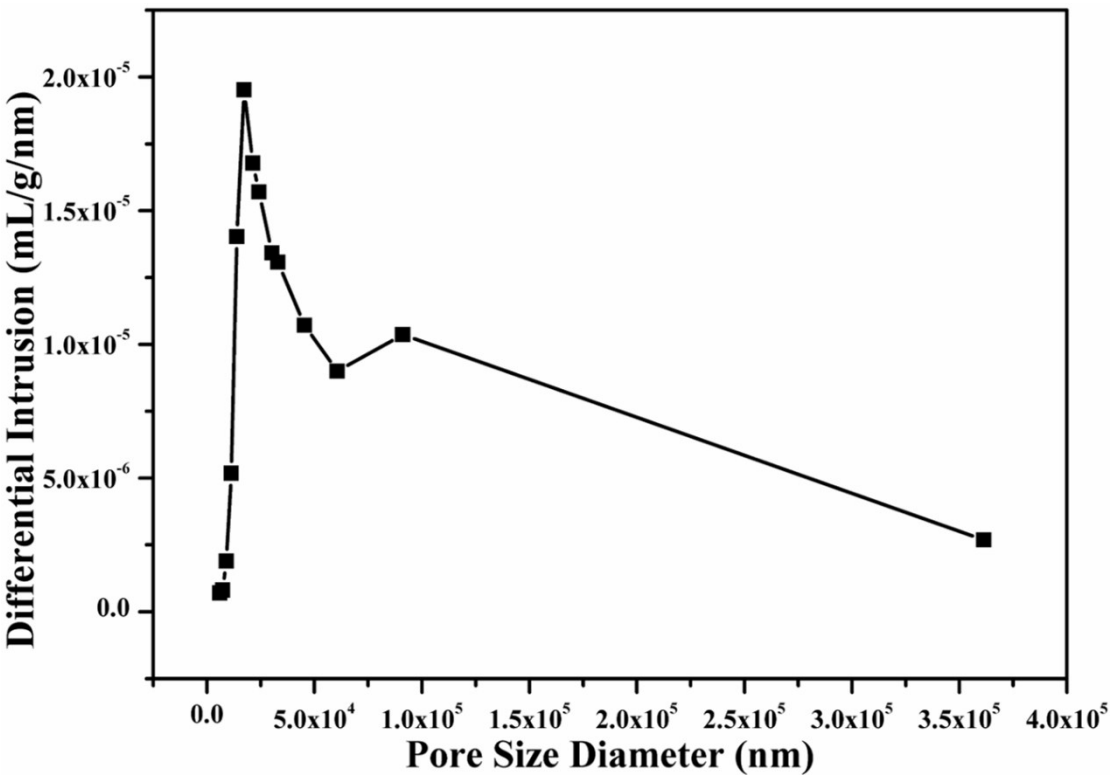

Figure S11. Pore diameter distribution of dried samples of the monolith d (c.f. Figure S7d).

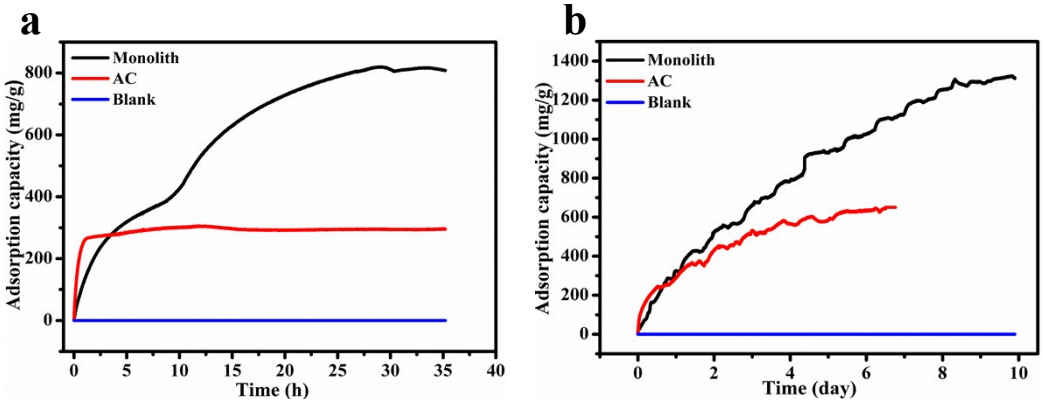

Figure S12. The real traces of the time-dependent adsorptions of the as prepared porous monolith (Figure S7d) and the commercially obtained ACs to (a) toluene and (b) formaldehyde.

Note: the blank for (a) is the monolith in air, and the blank for (b) is recorded with the presence of a small bottle of water.

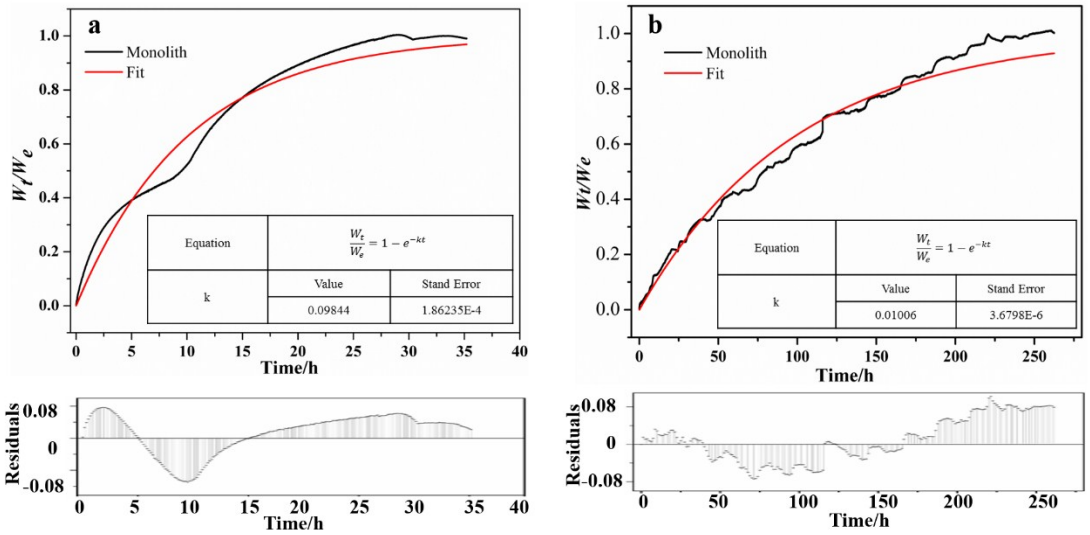

Figure S13. Variation of Wt/W_e versus time for toluene (a) and formaldehyde (b) adsorption on monolith **d** (c.f. figure S7).

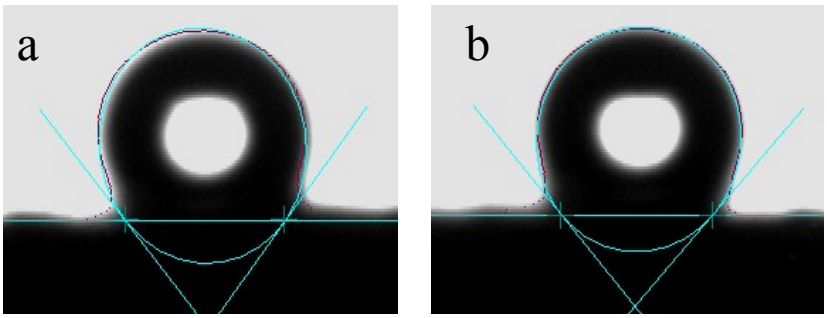

Figure S14. Images of contact angles of two porous materials with water, where (a, b) are the images of monoliths **c** and **d** (c.f. Figure S7), respectively.